Chinese Chemical Letters 34 (2023) 108251

Contents lists available at ScienceDirect

Chinese Chemical Letters

journal homepage: www.elsevier.com/locate/cclet

Insertion of unnatural metal ligand in the heme pocket of nitrophorin through protein semi-synthesis: Toward biomimicking binuclear active sites

Yonglu Chen[1], Yi Zhou[1], Chunmao He*

School of Chemistry and Chemical Engineering, South China University of Technology, Guangzhou 510640, China

ARTICLE INFO

Article history:
Received 1 January 2023
Revised 17 February 2023
Accepted 21 February 2023
Available online 28 February 2023

Keywords:
Protein semi-synthesis
Protein modification
Nitrophorin 2
Heteronuclear active site
Native chemical ligation

ABSTRACT

Herein, we report a semi-synthetic strategy affording a nitrophorin 2 (NP2) variant with a *N*,*N*′-bis(2-pyridylmethyl)amine (Dpa) ligand as sidechain selectively installed at position 27, which was assembled from a synthetic peptide thioester bearing the Dpa ligand and an expressed protein segment *via* native chemical ligation. The semi-synthetic NP2 was able to accept the natural heme *b* cofactor and the Dpa ligand was able to bind Cu(II)/Fe(III) ions, leading to heteronuclear active site.

Chemoselective protein modification is an important strategy for elucidation and manipulation of protein functions. To date, while challenging, protein modification at N- or C-terminus [1–3], side chains [4,5] and even backbone amides [6,7] have been achieved. Broadly speaking, two types of methods have been developed, *i.e.*, modification of canonical amino acids or non-canonical amino acids (ncAAs) that can be incorporated *via* genetic code expansion technology [8–11]. Meanwhile, protein semi-synthesis, where a large recombinantly expressed protein segment is ligated with a small peptide segment hosting the desired modification by selective ligation technologies, has been applied to offer a large number of proteins with natural post-translational modification patterns and protein bioconjugates [12–15].

Heme-copper oxidases (HCOs) and nitric oxide reductases (NORs) are essential in cell respiratory metabolism as they catalyze the multi-proton and multi-electron reduction of O_2 and NO, respectively [16–20]. These challenging life-essential reactions are facilitated at the heteronuclear active sites comprising a heme/copper (Cu_B) and a heme/non-heme iron (Fe_B) center for HCO and NOR, respectively (Figs. 1A and B). The elucidation of the role and mechanism of these heteronuclear sites in the catalytic cycle at molecular level has, however, been severely hampered by the large size (100–300 kDa) and complex structure (multiple subunits/metal-centers) of these membrane associated proteins [21]. To circumvent these restrictions, numerous synthetic models have been reported [21–23], but a consistent challenge in these small molecular models is to accurately mimic the long-range non-covalent interactions that may be important for enzymatic functions. To this end, several biosynthetic models have been developed. Notably, myoglobin (Mb) has been selected as a prime scaffold due to its small size and robust structure, and rationally-designed mutations have been exploited to mimic the functions of HCOs and NORs (Fig. 1C) [21,22,24–27]. Despite these successes, more diverse protein scaffolds that can be obtained with alternative strategies are warranted to complement the understanding of these essential enzymes.

Herein, we disclose our attempt to engineer binuclear centers (BNCs) into the nitrophorin (NP) scaffold. NPs are a family of heme *b* proteins identified in the saliva of the blood-sucking insect *Rhodnius prolixus*, and function as natural NO transport proteins [28,29]. NPs are lipocalin-like proteins with an eight-stranded β-barrel scaffold (Fig. 1D), and the hydrophobic distal pocket is larger enough to accommodate a variety of ligands, including imidazole and histamine [30–32]. Recently, we have established NP2 as a robust enzyme facilitating olefin cyclopropanation with excellent yield and stereo-selectivity [33], demonstrating the catalytic promiscuity of this group of protein scaffolds. More importantly, extensive mutations have been applied on NPs and the resulting structures are deposited in the protein database, making them ideal scaffold for biosynthetic modeling. In the present

---

* Corresponding author.
E-mail address: hecm@scut.edu.cn (C. He).

[1] These authors contributed equally to this work.

https://doi.org/10.1016/j.cclet.2023.108251

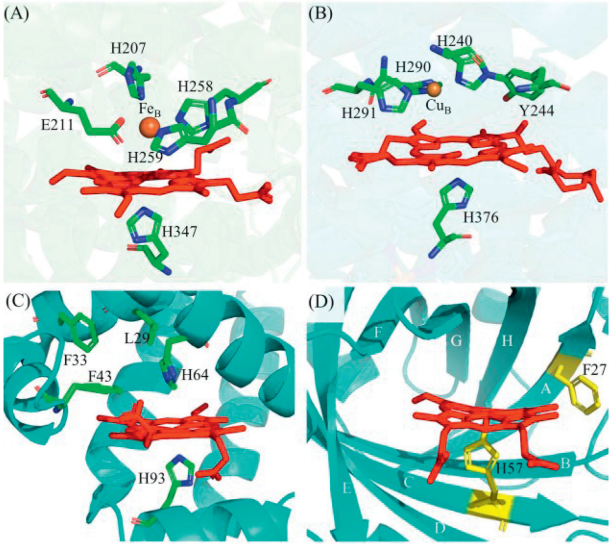

Fig. 1. Active site structures of (A) NOR with heme/Fe$_B$ (PDB code: 3O0R) and (B) HCO with heme/Cu$_B$ (PDB code: 5B1B). (C) Heme pocket of sperm whale Mb, highlighting key amino acid residues for engineering into HCO/NOR models (PDB code: 1VXA), (D) heme pocket of NP2, highlighting the site of mutation in this work, *i.e.*, F27 (PDB code: 1EUO).

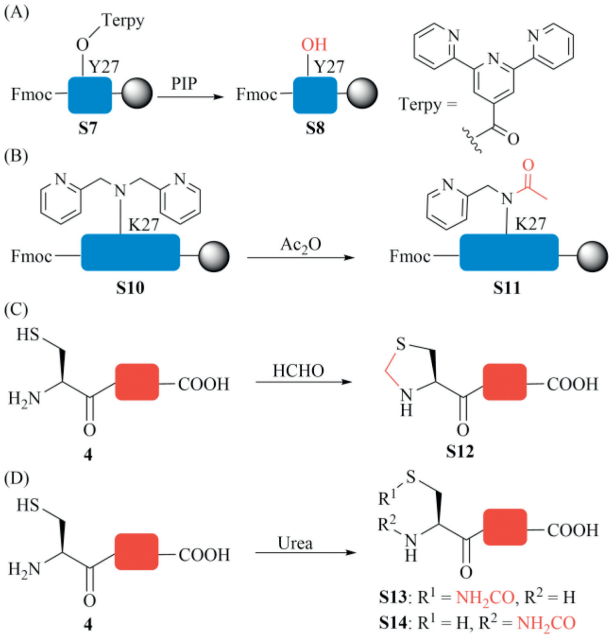

Fig. 2. Side-reactions observed in the synthesis of the two peptide segments (Blue, synthetic peptide segment; Red, expressed segment).

study, we chose to construct the BNC into the NP2 scaffold *via* protein semi-synthesis, which, as mentioned, combines the advantages of the efficiency of expressed protein segment and the selective-modification of the synthetic peptide segment.

For this purpose, Phe27, which is in the vicinity of heme cofactor, was selected as mutation site and a metal ligand was installed as a sidechain (Fig. 1D). In order to obtain the semi-synthetic NP2, Cys39 was selected as the ligation site, and the two peptide segments, *i.e.*, a synthetic peptide segment NP2 (1–38) with C-terminal thioester and an expressed Cys–peptide NP2 (39–179) **4**, can be linked by native chemical ligation (NCL) (Figs. 2 and 3) [34,35]. Initially, the tridentate terpyridine (terpy) motif, which exhibits high affinity to both Fe^{III} and Cu^{II}, was chosen as the ligand [36]. Therefore, a monomer where the terpy motif was attached to the sidechain of Tyr, Fmoc-L-Tyr(Terpy)-OH (**S4**, Figs. S1 and S2 in Supporting information), was synthesized and introduced to the NP2 (1–38) segment *via* standard solid phase peptide synthesis (SPPS). However, the monomer was completely destructed during the Fmoc deprotection process with piperidine (PIP) (Fig. 2A and Figs. S5 and S6 in Supporting information). Alternatively, we turned to the *N*,*N*′-bis(2-pyridylmethyl)amine (Dpa) ligand, which was extensively utilized in synthetic models [37]. Again, a monomer where the Dpa ligand was attached to the sidechain of Lys, Fmoc-L-Lys(Dpa)-OH (**S6**, Figs. S3 and S4 in Supporting information), was synthesized and introduced to the NP2 (1–38) segment. Unfortunately, a mass of −49 Da compared to the expected peptide was observed during the elongation (Fig. S7 in Supporting information), indicating the instability of the Dpa sidechain, possibly during the capping process with acetic anhydride (Fig. 2B) [38]. Lastly, we switched to an on-resin reductive amination strategy and it gave the final peptide **1** with the expected Dpa ligand, and importantly, it was stable during the trifluoroacetic acid (TFA) cleavage (Fig. S8 in Supporting information) [38]. Notably, the N-terminal Fmoc group in **1** was retained at this stage to facilitate a satisfactory high performance liquid chromatography (HPLC) purification.

Subsequently, efforts were made to obtain the expressed protein segment **4**, which was expressed with its C-terminal fused to a His$_6$-SUMO tag. Upon purification, the fusion protein was conveniently cleaved with SUMO-specific protease Ulp1 to offer segment **4** in 20 mg/L LB (Fig. 3D, Figs. S10 and S11 in Supporting information) [39,40]. It was noteworthy that two side reactions were observed during purification of peptide **4**: 1) Formation of tetrahydrothiazolane at the N-terminus with formaldehyde (Fig. 2C and Fig. S12 in Supporting information), which can be removed by incubation with *O*-methoxyamine at pH 4 [41]. 2) N-terminal carbamylation at either thiol or amine group by the denaturing agent urea (Fig. 2D and Fig. S13 in Supporting information) [42], which could be avoided by switching to guanidine-HCl (GdmCl).

With peptides **1** and **4** in hand, the following transformations leading to the full length protein were investigated (Fig. 3B). Firstly, the Fmoc deprotection and thioester transformation of segment **1**, and its ligation with segment **4** by NCL was attempted in one-pot. While the Fmoc removal of **1** with 20% PIP and the following thioester transformation with Dawson's acetylacetone activation of peptide hydrazide went smoothly to the desired thioester **3** (Fig. 3C and Fig. S14 in Supporting information) [43], and the ligation of **3** with peptide **4** was carried out in a one-pot to afford the full-length peptide **5** within 20 h (Fig. 3E and Fig. S15 in Supporting information).

To maximize the overall synthetic yield, the ligation mixture was reduced with excess tris(2-carboxyethyl)phosphine hydrochloride (TCEP) and the buffer exchanged to 6 mol/L GdmCl (pH 7), and it was directly subjected to refolding. However, most of the peptide materials precipitated out after one day (data not shown), which is a well-known phenomenon for the refolding of NPs. Alternatively, ligation product was purified with semi-preparative HPLC and the isolated yield of peptide **5** was 20.3%. After lyophilization, peptide **5** was redissolved in 6 mol/L GdmCl buffer (pH 7) and followed by addition into refolding buffer dropwisely at 4 °C. After one day, HPLC and electrospray ionization mass spectrometry (ESI-MS) analysis indicated the formation of the desired protein **6** (Fig. 4A and Fig. S16 in Supporting information). A loss of 4 Da in the mass of **6** compared to **5** was in good agreement with the formation of two disulfide bonds. The folded protein was finally concentrated and purified with size-exclusion chromatogram (SEC) (overall isolated yield of ligation and refolding: 6.7%). With the established protocol,

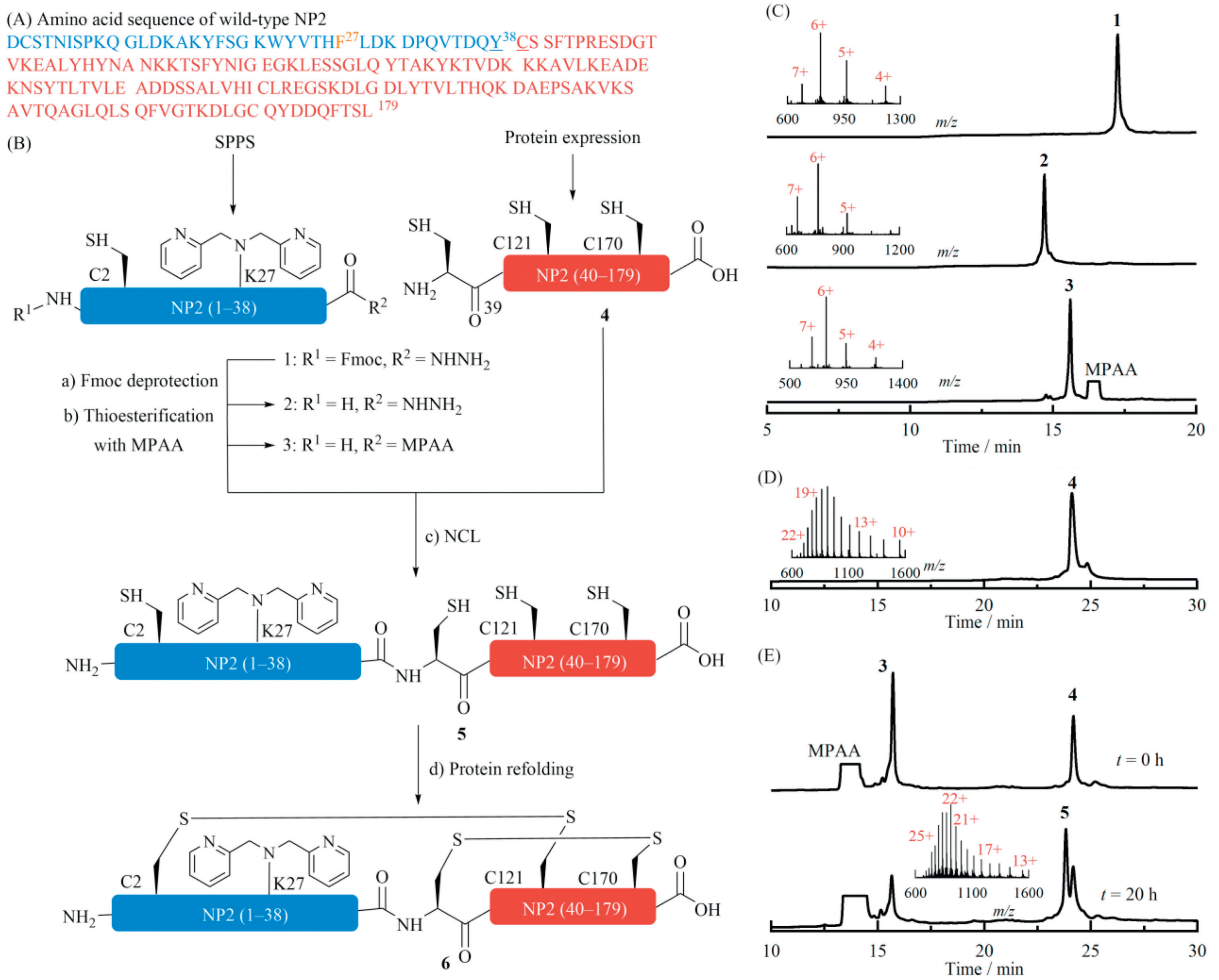

Fig. 3. (A) Amino acid sequence of wild-type NP2. The mutation site is marked in orange and the ligation site was underlined. (B) The semi-synthetic strategy of NP2-F27K(Dpa). (C) The analytical HPLC traces of **1**, its Fmoc deprotection, and thioesterification with MPAA. Inset: ESI-MS analysis of **1** (calc. 4824.2 Da, obsd. 4823.8 Da), **2** (calc. 4602.2 Da, obsd. 4601.1 Da) and **3** (calc. 4738.4 Da, obsd. 4737.5 Da). (D) The analytical HPLC trace of **4** after Ni immobilized metal-ion affinity chromatography (Ni-IMAC) purification. Inset: ESI-MS analysis of **4**. (calc. 15,515.2 Da, obsd. 15,513.0 Da). (E) The analytical HPLC traces of the NCL between peptide **3** and peptide **4**. Inset: ESI-MS analysis of **5** (calc. 20,085.1 Da, obsd. 20,083.5 Da).

10 mg of folded apo-protein **6**, *i.e.*, NP2-F27K(Dpa), can be obtained routinely, which is essential for further functional studies.

The heme *b* cofactor was titrated into **6** and the process was monitored by ultraviolet–visible (UV–vis) absorption spectroscopy. An absorption band at 403 nm appeared following the incorporation of heme *b* cofactor, agreeing well with the wild-type (wt) NP2 [44]. The reconstituted holoprotein was further purified by SEC to remove excess hemin (Fig. 4B and Fig. S17 in Supporting information). Next, 2 equiv. of Cu^{II} ions were further titrated into the heme-protein, which was followed by 2 h incubation to establish a full coordination of Cu^{II} by the Dpa ligand. ESI-MS and electron paramagnetic resonance (EPR) spectroscopic analysis showed the successful incorporation of Cu^{II}, *i.e.*, formation of NP2-F27K(Dpa-Cu^{II}) with a heme/Cu_B BNC (Fig. 4C and Fig. S19 in Supporting information). Moreover, in a control experiment, Fe^{III} titration was conducted for the apo-protein **6**, a small but appreciable absorbance at 371 nm was observed, indicating the formation of Dpa–Fe^{III} complex [45], *i.e.*, the formation of apo-NP2-F27K(Dpa-Fe^{III}) (Fig. 4D). Collectively, these data indicate that the semi-synthetic NP2 variant can be refolded properly to accept its natural heme *b* cofactor, more importantly, heteronuclear heme/Cu_B or heme/Fe_B centers can be engineered into the NP2 scaffold.

Further, DEA-NO, an NO releasing compound, was added to the semi-synthetic holo-NP2-F27K(Dpa), and the maximum absorbance shifted from 403 nm to 423 nm with concomitant formation of two Q-bands at 536 and 572 nm (Fig. S18 in Supporting information), indicating the formation of a Fe^{III}–NO complex, which is similar to the wt NP2 [46]. Lastly, NPs have been shown to able to catalyze the nitrite dismutation reaction [47]. To further probe the impact of the Dpa ligand on the structure and function of the semi-synthetic protein, the nitrite dismutase activities were compared between wt NP2, holo-NP2-F27K(Dpa), holo-NP2-F27K(Dpa-Cu^{II}) and holo-NP2-F27K(Dpa-Fe^{III}). As shown in Fig. 4E and Fig. S18 in Supporting information, similar k_{obs} values (*i.e.*, dismutase activities) were obtained in all cases. Altogether, it demonstrates clearly that the Dpa ligand has a minimum impact on the structure and function of the original NP2 scaffold. The HCO/NOR properties and catalytic functions of the semi-synthetic NP2 variant are under intensive investigation, and the results will be reported as they become available.

In summary, we have developed an efficient semi-synthesis method to build a biosynthetic BNC model on the NP2 scaffold, which, to the best of our knowledge, represent the first example of a semi-synthetic protein with a heteronuclear metal center. The Dpa ligand was selectively assembled by on-resin reductive amination at desired peptide sidechain, and in just one ligation the full-length protein segment was obtained. The Dpa-containing NP2 variant was able to refold to its native structure, after which,

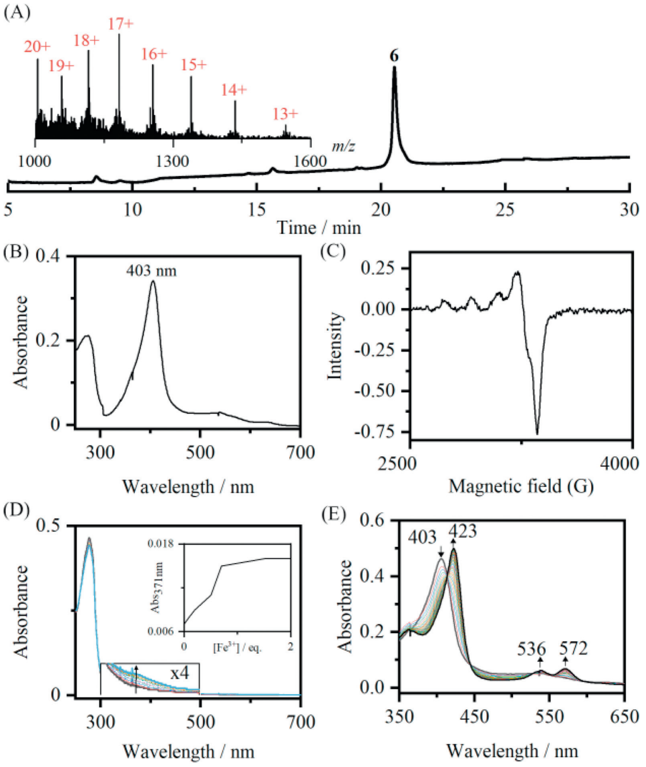

Fig. 4. (A) Analytical HPLC trace of **6**. Inset: ESI-MS analysis of **6** (calc. 20,081.3 Da, obsd. 20,077.1 Da). (B) UV–vis absorption spectrum of holoprotein NP2-F27K(Dpa). Protein conc. 2.4 μmol/L, in 0.1 mmol/L NaOAc, 0.1 mmol/L NaCl, 2% glycerol, pH 5.5. (C) X-band EPR spectrum of NP2-F27K(Dpa-Cu^{II}). Protein conc. 200 μmol/L, in 0.1 mol/L MOPS, 10% glycerin, pH 7.2, 100 K. (D) UV–vis absorption spectroscopy of Fe^{III} titration into apo-NP2-F27K(Dpa). Inset: The absorption at 371 nm upon addition of Fe^{III} ions. Protein conc. 21 μmol/L, in 0.1 mol/L NaOAc, 0.1 mol/L NaCl, pH 5.5. (E) The UV–vis absorption spectroscopy of the reaction of holoprotein NP2-F27K(Dpa) with $NaNO_2$. Protein conc. 3.3 μmol/L, in 0.1 mol/L NaH_2PO_4, 0.1 mol/L NaCl, pH 5.5, 1.7 mmol/L $NaNO_2$.

heme *b* cofactor and Cu/Fe ions were sequentially added to afford the BNC complexes, NP2-F27K(Dpa-Cu^{II}) or F27K(Dpa-Fe^{III}). It establishes that protein semi-synthesis is a viable technology in installing protein modifications site-specifically, and in this case, a metal ligand Dpa was selectively incorporated into NP2 scaffold. With this strategy, one can imagine easily changing the type of ligand or choosing other modification sites, which would greatly expand the scope and applicability of semi-synthetic NP2 model proteins.

Declaration of competing interest

The authors declare that they have no known competing financial interests or personal relationships that could have appeared to influence the work reported in this paper.

Acknowledgments

The financial support from the National Natural Science Foundation of China (Nos. 22077036 and 22277029) is greatly acknowledged. We also thank Shunzhi Huang, Junlang Chen, Xiaoxin Yin and Jun Wang of the group for helpful discussion.

Supplementary materials

Supplementary material associated with this article can be found, in the online version, at doi:10.1016/j.cclet.2023.108251.

References

[1] C.B. Rosen, M.B. Francis, Nat. Chem. Biol. 13 (2017) 697–705.
[2] S. Bloom, C. Liu, D.K. Kölmel, et al., Nat. Chem. 10 (2018) 205–211.
[3] H. Jiang, W. Chen, J. Wang, R. Zhang, Chin. Chem. Lett. 33 (2022) 80–88.
[4] O. Boutureira, G.J.L. Bernardes, Chem. Rev. 115 (2015) 2174–2195.
[5] Y. Yang, M. Liang, R. Wang, C. He, Chin. Chem. Lett. 34 (2023) 107806.
[6] J. Yang, C. Wang, S. Xu, J. Zhao, Angew. Chem. Int. Ed. 58 (2019) 1382–1386.
[7] J. Ohata, S.C. Martin, Z.T. Ball, Angew. Chem. Int. Ed. 58 (2019) 6176–6199.
[8] A.D. Pagar, M.D. Patil, D.T. Flood, et al., Chem. Rev. 121 (2021) 6173–6245.
[9] S. Xu, Z. Zhao, J. Zhao, Chin. Chem. Lett. 29 (2018) 1009–1016.
[10] X. Ling, H. Chen, W. Zheng, et al., Chin. Chem. Lett. 31 (2020) 163–166.
[11] S. Lin, C. He, Chin. Chem. Lett. 29 (2018) 1017–1021.
[12] R.E. Thompson, T.W. Muir, Chem. Rev. 120 (2020) 3051–3126.
[13] C.P.R. Hackenberger, D. Schwarzer, Angew. Chem. Int. Ed. 47 (2008) 10030–10074.
[14] J. Zhao, J. Liu, X. Liu, et al., Chin. J. Chem. 40 (2022) 787–793.
[15] F. Ye, J. Zhao, P. Xu, et al., Angew. Chem. Int. Ed. 60 (2021) 12904–12910.
[16] S. Ferguson-Miller, G.T. Babcock, Chem. Rev. 96 (1996) 2889–2908.
[17] G.T. Babcock, Proc. Natl. Acad. Sci. U. S. A. 96 (1999) 12971–12973.
[18] G.T. Babcock, M. Wikström, Nature 356 (1992) 301–309.
[19] J. Oost, A.P.N. Boer, J.W.L. Gier, et al., FEMS Microbiol. Lett. 121 (1994) 1–9.
[20] I.M. Wasser, S. de Vries, P. Moënne-Loccoz, I. Schröder, K.D. Karlin, Chem. Rev. 102 (2002) 1201–1234.
[21] C.J. Reed, Q.N. Lam, E.N. Mirts, Y. Lu, Chem. Soc. Rev. 50 (2021) 2486–2539.
[22] S.M. Adam, G.B. Wijeratne, P.J. Rogler, et al., Chem. Rev. 118 (2018) 10840–11022.
[23] E. Kim, E.E. Chufán, K. Kamaraj, K.D. Karlin, Chem. Rev. 104 (2004) 1077–1134.
[24] A. Bhagi-Damodaran, I. Petrik, Y. Lu, Israel J. Chem. 56 (2016) 773–790.
[25] J.A. Sigman, B.C. Kwok, Y. Lu, J. Am. Chem. Soc. 122 (2000) 8192–8196.
[26] N. Yeung, Y. Lin, Y. Gao, et al., Nature 462 (2009) 1079–1082.
[27] J.A. Sigman, H.K. Kim, X. Zhao, J.R. Carey, Y. Lu, Proc. Natl. Acad. Sci. U. S. A. 100 (2003) 3629–3634.
[28] F.A. Walker, J. Inorg. Biochem. 99 (2005) 216–236.
[29] J.M.C. Ribeiro, J.M.H. Hazzard, R.H. Nussenzveig, D.E. Champagne, F.A. Walker, Science 260 (1993) 539–541.
[30] C. He, K. Nishikawa, Ö.F. Erdem, et al., J. Inorg. Biochem. 122 (2013) 38–48.
[31] A. Weichsel, J.F. Andersen, D.E. Champagne, F.A. Walker, W.R. Montfort, Nat. Struct. Mol. Biol. 5 (1998) 304–309.
[32] C. He, H. Ogata, M. Knipp, Biochemistry 49 (2010) 5841–5851.
[33] S. Huang, W. Deng, R. Liao, C. He, ACS Catal. 12 (2022) 13725–13731.
[34] P.E. Dawson, T.W. Muir, I. Clark-Lewis, S.B.H. Kent, Science 266 (1994) 776–779.
[35] S.B.H. Kent, Chem. Soc. Rev. 38 (2009) 338–351.
[36] C. Wei, Y. He, X. Shi, Z. Song, Coord. Chem. Rev. 385 (2019) 1–19.
[37] D.W. Brogden, J.F. Berry, Comments Inorg. Chem. 36 (2016) 17–37.
[38] Y. Zhou, Y. Chen, C. He, Dalton Trans. 50 (2021) 4231–4236.
[39] P. Liao, H. Liu, C. He, Chem. Sci. 13 (2022) 6322–6327.
[40] M.P. Malakhov, M.R. Mattern, O.A. Malakhova, et al., J. Struct. Func. Genom. 5 (2004) 75–86.
[41] I.E. Gentle, D.P. De Souza, M. Baca, Bioconjug. Chem. 15 (2004) 658–663.
[42] S. Sun, J. Zhou, W. Yang, H. Zhang, Anal. Biochem. 446 (2014) 76–81.
[43] D.T. Flood, J.C.J. Hintzen, M.J. Bird, et al., Angew. Chem. Int. Ed. 57 (2018) 11634–11639.
[44] Y. Zhang, J.M.C. Ribeiro, J.A. Guimarães, P.N. Walsh, Biochemistry 37 (1998) 10681–10690.
[45] J. Mukherjee, V. Balamurugan, R. Gupta, R. Mukherjee, Dalton Trans. 19 (2003) 3686–3692.
[46] J.F. Andersen, X.D. Ding, C. Balfour, et al., Biochemistry 39 (2000) 10118–10131.
[47] C. He, M. Knipp, J. Am. Chem. Soc. 131 (2009) 12042–12043.